

The performance of the ATLAS Level-1 Calorimeter Trigger with LHC collision data

Juraj Bracinik^a on behalf of the ATLAS collaboration

^aUniversity of Birmingham, United Kingdom

E-mail: jrb@hep.ph.bham.ac.uk

ABSTRACT: The ATLAS first-level calorimeter trigger is a hardware-based system designed to identify high- E_T jets, electron/photon and τ candidates and to measure total and missing E_T in the ATLAS calorimeters. After more than two years of commissioning in situ with calibration data and cosmic rays, the system has now been used extensively to select the most interesting proton-proton collision events. Fine tuning of timing and energy calibration has been carried out in 2010 to improve the trigger response to physics objects. In these proceedings, an analysis of the performance of the level-1 calorimeter trigger is presented, along with the techniques used to achieve these results.

KEYWORDS: ATLAS; LHC; Trigger.



Contents

1. Introduction	1
2. Calibration of the system	1
3. Experience from data taking and efficiency for triggering of physics objects	4

1. Introduction

Triggering at LHC is difficult. While the total interaction cross section is of the order of 10 mb, the cross section for discovery physics is many orders of magnitude smaller. To cope with this challenge, ATLAS has built a three level trigger system, with two levels (Level-2 and Level-3) implemented in software, and the Level-1 system implemented in custom built hardware. The Level-1 Trigger consists of several components, among them the Level-1 Muon trigger, Level-1 Calorimeter trigger (L1Calo) and Central Trigger Processor.

L1Calo [1] selects events by looking for hard final state objects, for example e/γ , τ or jets that lead to localized energy deposits, or for global event properties such as E_T and missing E_T . It is implemented as a pipelined, synchronous system, with fixed latency of up to $2.5 \mu s$. It has several processing stages, and profits from large-scale parallel processing. Most of the electronics is custom made, mainly FPGA based, consisting of around 300 VME modules of 10 types housed in 17 crates. The system was installed at the end of 2007, taking cosmic data for commissioning and detailed checks of L1Calo performance in 2008 and part of 2009, followed by early beam data, taken at the end of 2009. Since early 2010 we have seen a gradual increase in delivered luminosity and several stepwise updates of L1Calo calibrations.

2. Calibration of the system

Conditioning and calibration of signals in L1Calo is done in several steps. Analogue signals are summed to Trigger Towers on the detector and then sent on twisted-pair cables to analogue receivers. Here analogue gains are applied, giving the first step in energy calibration. The signals are then digitized and aligned in time, and passed to a digital (FIR) filter. The FIR filter assigns the signal to the correct bunch-crossing, its output is fed into a Look-Up table (LUT), where pedestal subtraction, noise suppression and the final step in energy calibration are done. Most of the steps in this calibration procedure are highly interdependent and adjustment of the calibration parameters is an iterative procedure. In the following, three important steps in the L1Calo calibration procedure will be discussed.

Analogue signals are routed from the calorimeter front-end to L1Calo electronics on twisted-pair cables with lengths varying between 30 and 70 meters, the difference in signal propagation

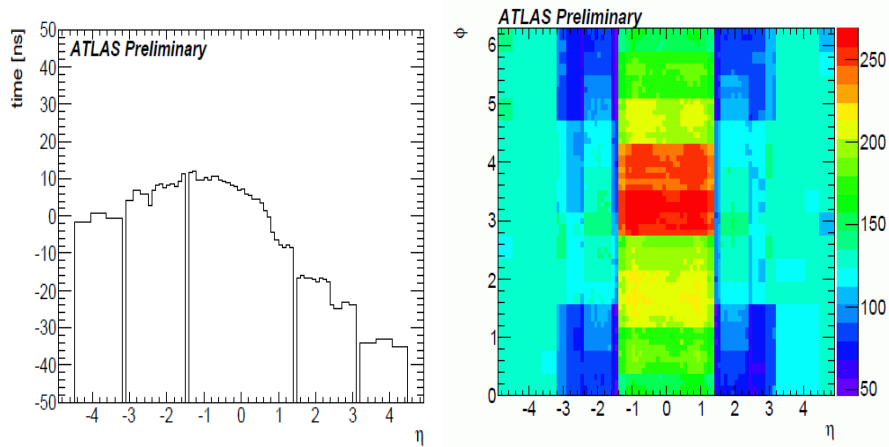


Figure 1. Trigger timing for splash events. The distribution of pulse maxima in EM layer for a splash event coming from high η side (left), total delays after correcting splash timing for time-of-flight effect (right).

time being of the order of 10 bunch crossings (BC)¹. It is necessary to align the signals at the input of L1Calo, as large mistiming leads to events being lost and smaller timing discrepancies lead to energy underestimation. There are several parameters available to adjust timing. Input delays (implemented in input FIFO) allow the alignment of signals with a step of 1 BC, fine timing (implemented in custom PHOS4 chip) allows the signal strobe timing to be adjusted in steps of 1 ns, and lastly the readout pointer determines which part of the pipeline is read out for events that were accepted.

A first approximation to L1Calo timing has been obtained using calorimeter calibration pulser systems, set up to mimic collisions. In a set of dedicated runs, the readout pointers are adjusted, the signals are aligned in input FIFO and the fine timing is adjusted in such a way that signals are strobed at pulse maximum. The second approximation to timing has been done using splash events, taken at the beginning of 2009 and 2010 data-taking periods. Splash events occur when the LHC beam hits a collimator, leading to large energy deposits in the whole ATLAS detector. These events are ideal for the timing adjustment, although it is necessary to correct for time-of-flight effects, as the particles do not come from the usual interaction point, but from upstream of the detector. Indeed, when good signals are selected and fitted with a function describing the expected signal shape, the time-of-flight effects are clearly seen (the distribution of signal maxima in EM layer for a splash event coming from the right hand side is shown in Fig. 1 left). After correcting for time-of-flight effects, total delays as used for early datataking are obtained (see Fig. 1 right). With increasing LHC luminosity, a further correction, determined using fits to collision signals is implemented, leading to timing known for most channels with a precision of ± 2 ns.

As typical signals from ATLAS calorimeters are several BCs long, it is necessary to attribute each energy deposit to a unique beam crossing. Also, it is reasonable to use more than one FADC sample for the energy measurement. In the case of L1Calo both of these functions are performed by a Finite Impulse Response (FIR) filter. Five FADC samples are multiplied by constant coefficients

¹The time between two LHC bunch crossings is 25 ns, equivalent to a frequency of 40 MHz.

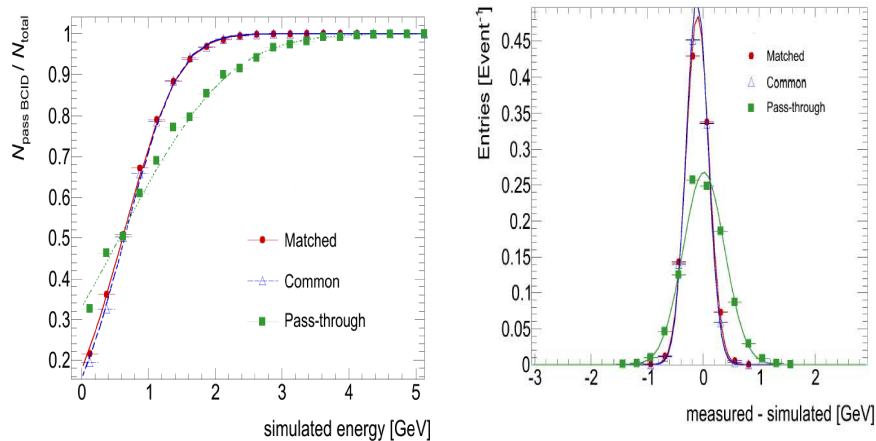


Figure 2. Comparison of performance for three sets of FIR filter coefficients (matched, common and pass-through filter), studied using calibration pulses superimposed on realistic noise. The efficiency for pulses to be attributed to the correct bunch crossing is shown on the left, the energy resolution for 25 GeV pulses is shown on the right.

c_i and summed together: $S = \sum_i c_i \times FADC_i$. The bunch crossing for which the sum is a maximum defines the time of the interaction². The value of the sum is used as the input to the LUT, and the LUT output gives the final calibrated E_T . The performance is expected to be best for the filter that is matched to the shape of the signal in each electronics channel. This is difficult to achieve, as tuning the filter parameters for each trigger tower would add significant complexity to the system. The performance of the FIR filter has been studied using calibration pulses superimposed on realistic noise, with results shown on Fig. 2. Three sets of FIR filter coefficients were studied, one consisting of coefficients tuned to the shape of calibration pulses in each tower (matched filter), one with coefficients adjusted for each calorimeter area (em layer, had layer and forward calorimeters, common filter) and one using the central BC only (pass-through filter). As can be seen, matched and common filters have better efficiency for attributing small pulses to the correct bunch crossing than pass-through filter (Fig. 2 left); they also lead to better energy resolution (Fig. 2 right). On the other hand, the difference in performance between matched and common filters is marginal. That is why L1Calo now uses a common filter.

The number of ADC counts seen in a trigger tower does not immediately translate to transverse energy in GeV³: it is necessary to introduce an energy calibration. Calibration coefficients are implemented in analogue gains in the receivers and in the slope of the LUT. The L1Calo system is calibrated in dedicated pulser runs, using the more precise energy measurement in the calorimeters. Several energy (calibration pulse amplitude) steps are taken in each calibration run, and gains are then determined by comparing the energy seen in the calorimeters and in L1Calo. The gains are loaded into the hardware and checked using LHC collision data.

²A different method is used for pulses that saturate the FADC scale.

³Although the approximate relation 1 ADC count \simeq 0.25 GeV holds.

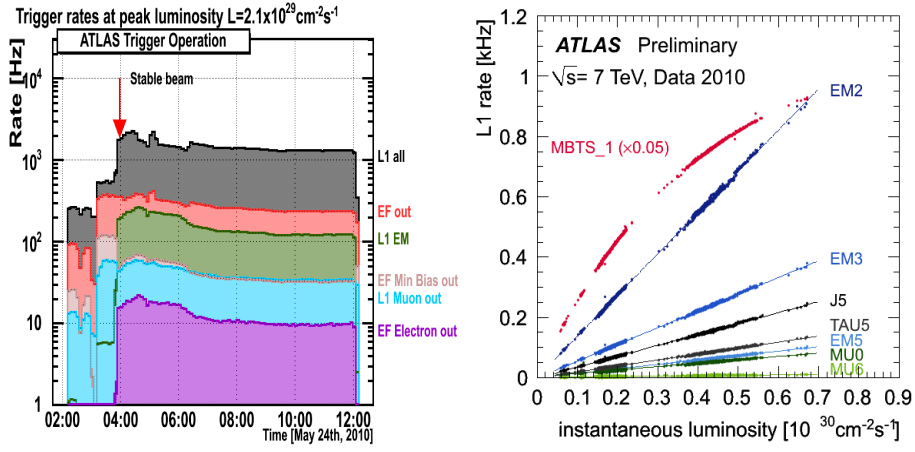


Figure 3. Trigger rates during typical LHC fill as a function of time (left). The figure shows total L1 rate (L1 all) and the sum of rates for L1 electromagnetic triggers (L1 em). L1 rates are reduced by the High Level Trigger (EF Out and EF Electron out). Rates of L1 triggers as a function of instantaneous luminosity (right) for several electromagnetic (EM2, EM3, EM5), τ (TAU5) and jet (J5) triggers.

3. Experience from data taking and efficiency for triggering of physics objects

L1Calo is largely a digital system and it is vital that it works without any digital errors. For accepted events the information passing through L1Calo is recorded as it is seen at different points in the algorithmic processing. This provides a possibility to check digital consistency by comparing this redundant readout with a detailed, bit-by-bit simulation that starts from raw ADC counts and models (recalculates) all steps in the chain. During data taking, the comparison is done on-line for a fraction of events, and offline for all events that were accepted by the ATLAS trigger system. No digital errors are tolerated: all rare occurrences of digital errors were traced to faulty modules or components which were replaced immediately.

Fig. 3 left shows trigger rates during a typical LHC fill. The data taking is very smooth, and rate excursions are rare. Rates of L1Calo triggers follow nicely the luminosity profile of the fill, and are reduced by another order of magnitude by the High Level Trigger. Fig. 3 right shows rates of several L1Calo triggers as a function of instantaneous luminosity. A nice linear dependence between trigger rates and luminosity is seen, showing that the contribution of electronics noise to L1 trigger rates is negligible, the rates being caused mainly by QCD collision background.

The quality of a trigger is visible when looking at trigger efficiencies for identified physics objects. Trigger efficiencies are also the interface between the detector and physics analysis. Fig. 4 shows trigger efficiencies defined as a ratio between the number of physics objects that were triggered by a given trigger and the number of all physics objects in given data sample. In order to avoid bias, the data sample should be triggered by an independent trigger, in this case Minimum Bias Trigger Scintillators [2]. In Fig. 4 left the trigger efficiency for electromagnetic clusters is shown as a function of offline cluster E_T for Level-1 trigger threshold EM5. This notation means that the energy of the cluster as seen by L1Calo should be bigger than 5 counts at the output of the LUT. This is roughly equivalent to 5 GeV and the point where the trigger efficiency starts to

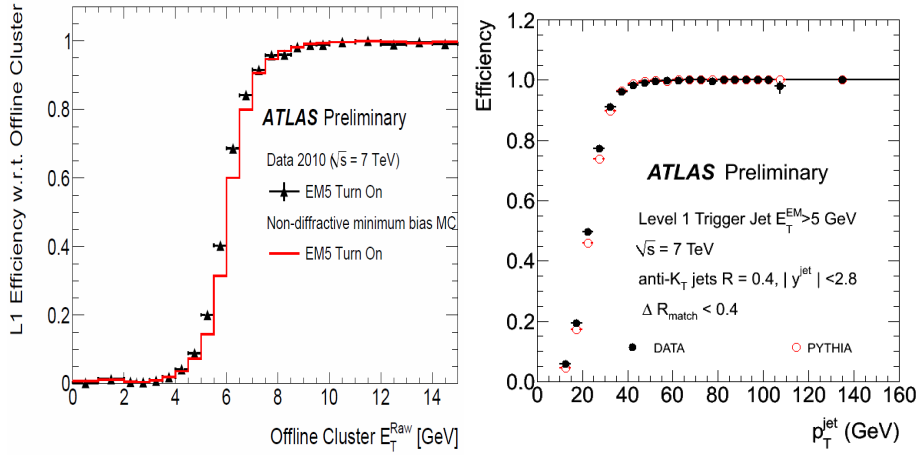


Figure 4. Trigger efficiency for physics objects, defined as a ratio between number of objects that passed the trigger and number of all reconstructed objects. The efficiency for electromagnetic clusters passing threshold EM5 is shown on the left and jets passing thresholds J5 is shown on the right.

rise from zero⁴. Full efficiency is reached at E_T of 8 GeV, with the steepness of the turn-on curve determined by the level of noise suppression cuts which are harder in trigger than offline, and by the probability that only part of offline cluster gets collected into L1 object. The efficiency turn-on curve is well described by Monte-Carlo simulation. In Fig. 4 right the trigger efficiency for offline reconstructed jets is shown as a function of the jet E_T for L1 trigger threshold J5. As in the case of electromagnetic clusters, the efficiency becomes greater than zero close to 5 GeV, while full efficiency is reached at E_T close to 40 GeV. As jets are usually broader objects than electromagnetic clusters, both effects of noise cuts and of possible energy leakage from L1 clusters are increased. In addition, the L1 jet energy is calculated using a "raw" electromagnetic scale, without corrections for dead material. As in the case of electromagnetic clusters, the trigger efficiency for jets is very well described by the Monte-Carlo simulation.

Acknowledgments

I would like to thank M. Watson and S. Hillier for their help with the talk and proceedings.

References

- [1] R. Achenbach et al., *The ATLAS Level-1 Calorimeter Trigger*, *JINST* **3** (2008) P03001 (ATL-DAQ-PUB-2008-001).
- [2] Tim Martin on behalf of ATLAS collaboration, *Development and Online Operation of Minimum Bias Trigger in ATLAS*, these proceedings.

⁴The trigger uses a condition $E_T > \text{threshold}$.